

Optimizing photovoltaic system performance through MPPT synergetic adaptive control

Kamel Hadjadj, Hadjira Attoui

QUERE Laboratory, Faculty of Technology, University of Setif 1, Setif, Algeria

Article Info

Article history:

Received Mar 28, 2024

Revised Nov 5, 2024

Accepted Nov 11, 2024

Keywords:

P&O algorithm

Photovoltaic system

Power transfer optimization

Synergetic adaptive control

Maximum power point tracking

ABSTRACT

This paper investigates enhancement of energy conversion through the implementation of new MPPT control strategy based on synergetic adaptive control (SAC) for a photovoltaic system. The architecture of this system encompasses a photovoltaic module, a DC-DC boost converter, a resistive load, and an MPPT controller. The controller amalgamates two distinct methodologies: the initial algorithm deduces the peak power current through a perturbation and observation (P&O) method, which serves as the reference point for the subsequent algorithm founded on synergetic adaptive control. The parameters for the latter are refined through the particle swarm optimization (PSO) technique. This innovative method is employed to ascertain the optimal power output across varying weather conditions, aiming to enhance power transmission performance irrespective of meteorological variations. The efficacy of this strategy was affirmed through a comparative study with the conventional P&O method using MATLAB/Simulink simulations, which verified the superior performance of the proposed algorithm.

This is an open access article under the [CC BY-SA](https://creativecommons.org/licenses/by-sa/4.0/) license.



Corresponding Author:

Kamel Hadjadj

QUERE Laboratory Faculty of Technology, University of Setif 1

19000 Setif, Algeria

Email: kamel.hadjadj@univ-setif.dz

1. INTRODUCTION

The problem of energy and its purity represents the most prominent challenges for the coming decades, owing to its profound implications for human existence across a spectrum of domains, ranging from economic prosperity to leisure activities. Fossil fuels continue to dominate the global energy landscape due to their proven effectiveness. However, their status as non-renewable sources, coupled with their detrimental environmental impacts, have prompted scientists to engage in the pursuit of efficient, sustainable and cleaner sources of energy. Renewable energies are the most important alternative to fossil fuels. Therefore, countries are racing to develop an effective, clean, and renewable source to ensure energy security in the future. The interest in alternative renewable energy sources, including wind, wave, and photovoltaic power, is increasing significantly.

Photovoltaic energy stands out as a crucial technology being advanced as an alternative energy source. The working principle of this technology is straightforward: it converts light into electrical energy. Among its advantages are its cost-effectiveness, relatively low environmental impact, and straightforward maintenance requirements. Photovoltaic generators are known to have several issues, including non-linear behavior, which means that there will be a loss in the generated energy because it is not proportional to the weather condition. Consequently, an algorithm is employed to monitor the peak power via an adaptation

phase, a process known as maximum power point tracking MPPT. The initial methods employed for MPPT tracking are referred to as classical techniques.

Among the classic techniques is perturbation and observation (P&O) [1], [2], which is characterized by disrupting the operating voltage and monitoring the resulting power. In contrast, hill climbing depends on a disturbance in the duty cycle [3]. Another method is incremental conductance (IC) [4], [5]. This method hinges on the premise that maximum power point (MPP) is achieved when the derivative of the power curve with respect to voltage is zero. Contemporary strategies utilizing artificial intelligence for MPP tracking have been formulated, encompassing fuzzy logic controllers (FLC) [6], [7], artificial neural network (ANN) [8], [9], neuro-fuzzy controller (NFC) [10]. These advanced algorithms have significantly enhanced the efficiency of MPP tracking, albeit at the cost of increased complexity and the necessity for a detailed understanding of the system's dynamics.

In the past few years, metaheuristic algorithms like particle swarm optimization (PSO) [11], [12], genetic algorithm (GA) [13], [14], and grey wolf optimization (GWO) [15], [16] have been innovated for optimal power extraction, aiming to converge accurately towards the MPP. These algorithms have demonstrated effectiveness in MPP tracking, yet their practical application may be complex. Nonlinear control also had its share in tracking the MPP. We find, for example, that sliding mode [17], [18] was relied upon by using the slope of the force vs the voltage curve as a sliding surface. This algorithm is characterized by its robustness and ease of implementation. However, its operation is still hindered by the shattering phenomenon.

Backstepping control was also employed to track the MPP [19]. It was refined by incorporating integration and sliding mode techniques, leading to the development of the integral backstepping sliding mode control (IBSMC) [20]. This enhancement minimizes the discrepancy between the produced current and the reference MPPT current. Furthermore, synergetic control, known for its nonlinear nature and rapid dynamic response [21]-[23]. It is distinguished from sliding mode by the absence of shattering phenomenon in its response. This paper introduces a new MPPT control strategy for photovoltaic systems, employing a synergetic adaptive methodology. This strategy is divided into two segments, with the initial segment dedicated to ascertaining the maximum current value generated by the photovoltaic panel through the P&O algorithm.

This specific value is used as a reference for the second part, which is synergetic adaptive control. This algorithm gives the difference between the generated current and the calculated reference to zero. To demonstrate the effectiveness of the proposed algorithm, a comparative study was conducted with the conventional P&O algorithm, illustrating the significant strength factors of the new method.

The structure of this paper is organized as follows: section 2 provides a concise overview of the photovoltaic generator. Section 3 details the mathematical model of the DC-DC boost converter. In section 4, the proposed algorithm, named the adaptive synergetic MPPT controller, is discussed. Section 5 delineates the simulation outcomes and a comparative analysis demonstrating the efficacy of the proposed method. The paper concludes with a summary in the final section.

2. PHOTOVOLTAIC GENERATOR

Photovoltaic panels are used in several forms depending on the needs. For example, they can be connected to the grid [24] or used in pumping systems. They are also used in stand-alone systems. A stand-alone system consists of (a) photovoltaic panel, (b) DC-DC boost converter, (c) resistive load, and (d) a controller. A photovoltaic panel is an electrical energy generator that converts light rays into a continuous electrical current. Utilizing the photovoltaic generator directly results in significant power loss when there are changes in irradiance or temperature [25], attributed to the non-linear characteristics of the photovoltaic panel. Consequently, a DC-DC boost converter is employed to maximize the voltage extraction from the photovoltaic generator.

Equivalent circuit model of photovoltaic cell used is the single-diode model illustrated in Figure 1. The equivalent circuit consist of photon generated current, anti-parallel diode, a parallel shunt resistance R_{sh} , and a serie resistance R_s . The output PV current can describe as:

$$I_{pv} = I_{ph} - I_d - I_{sh} \quad (1)$$

$$I_{sh} = \frac{V_{pv} + I_{pv}R_s}{R_{sh}} \quad (2)$$

$$I_d = I_0 \left[\exp \left(q \frac{V_{pv} + I_{pv}R_s}{AKT} \right) - 1 \right] \quad (3)$$

$$I_0 = I_{0r} \left(\frac{T}{T_r}\right)^3 \exp\left(\left[\frac{qE_g}{AK}\right] \times \left[\frac{1}{T_r} - \frac{1}{T}\right]\right) \tag{4}$$

$$I_{ph} = G[I_{sc} + K_i(T - T_r)] \tag{5}$$

The output PV current given by:

$$I_{pv} = I_{ph} - I_0 \left[\exp\left(q \frac{V_{pv} + I_{pv}R_s}{AKT}\right) - 1 \right] - \frac{V_{pv} + I_{pv}R_s}{R_{sh}} \tag{6}$$

Here:

I_{pv} is the output PV current

V_{pv} is the output PV voltage

I_{ph} is a photocurrent

I_{sh} is a shunt current

I_d is the dark current

I_0 is the reserved saturation current

K is Boltzmann's constant

q is the charge of an electron

E_g stands for the energy of the band gap for silicon

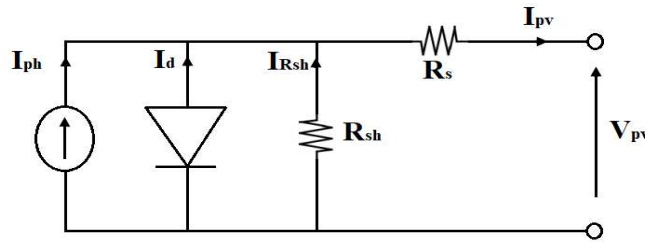


Figure 1. Equivalent circuit of PV cell

The photovoltaic panel is modeled with parameter values of ET-M572185, as shown in Table 1.

Figures 2 and 3 depict the power-voltage and current-voltage characteristics under varying levels of irradiance while maintaining a constant temperature ($T = 25\text{ }^\circ\text{C}$), respectively. Conversely, Figures 4 and 5 display the power-voltage and current-voltage curves across various temperatures, with a steady irradiance level ($G = 1,000\text{ W/m}^2$).

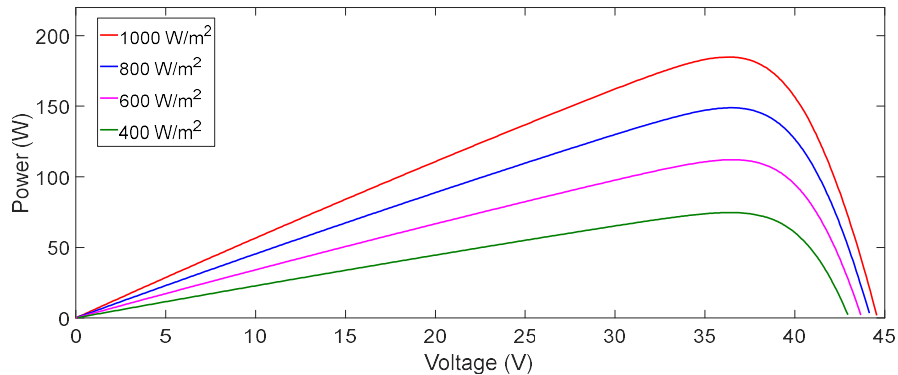


Figure 2. Power-voltage curve under different irradiance levels ($T = 25\text{ }^\circ\text{C}$)

Table 1. Specification of PV array panel

Electrical parameters of PV system	Value
Maximum power Pmax	184.767 (W)
Open circuit voltage Voc	44.6 (V)
Short circuit current Isc	5.8 (A)
Voltage at maximum power point Vmp	36.3 (V)
Current at maximum power point Imp	5.09 (A)

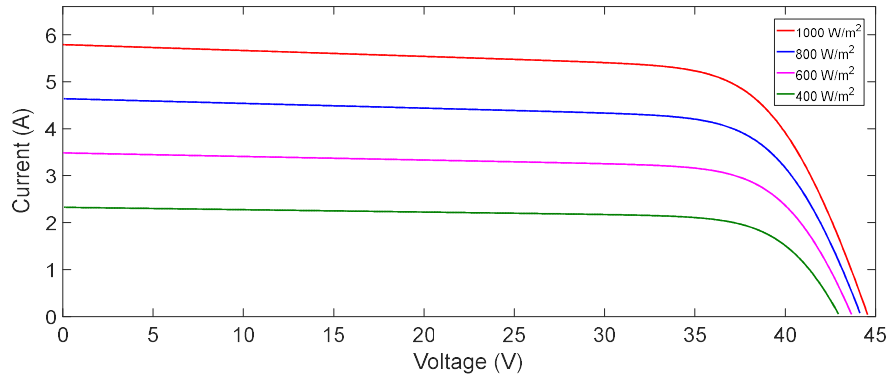


Figure 3. Current-voltage curve under different irradiance levels ($T = 25\text{ }^{\circ}\text{C}$)

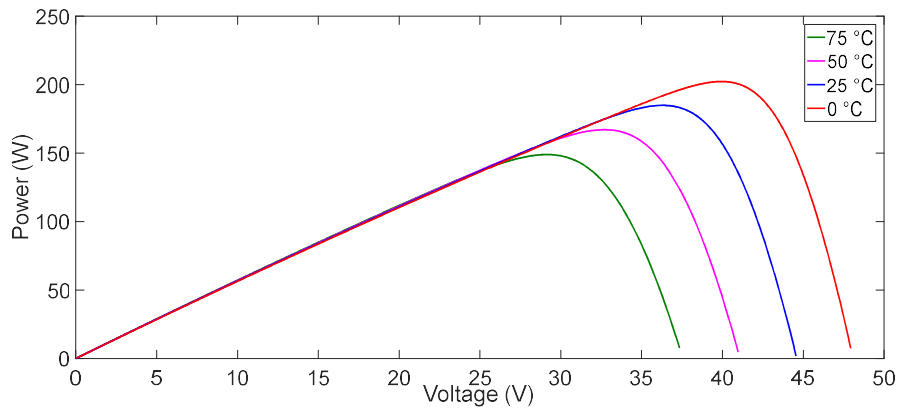


Figure 4. Power-voltage curve under different temperatures ($G = 1,000\text{ W/m}^2$)

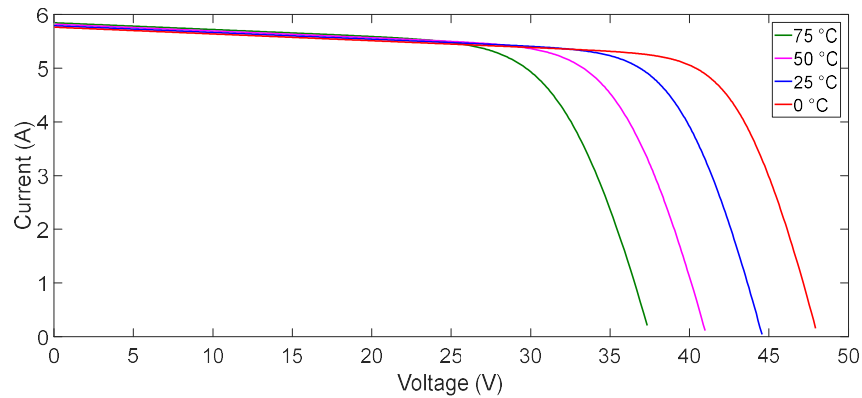


Figure 5. Current-voltage curve under different temperature ($G = 1,000\text{ W/m}^2$)

3. DC-DC BOOST CONVERTER

DC-DC boost converter acts as an intermediary between the photovoltaic panel and the resistive load, facilitating the tracking of the maximum power point regardless of fluctuations in weather conditions. Its operation is governed by a pulse-width modulation PWM signal, controlled through switch S. The boost converter can be described as:

$$\frac{dV_{pv}}{dt} = \frac{I_{pv}}{C_r} - \frac{i_l}{C_r} \quad (7)$$

$$\frac{di_l}{dt} = -(1-d)\frac{V_0}{L} + \frac{V_{pv}}{L} \quad (8)$$

$$\frac{dV_0}{dt} = (1-d)\frac{i_l}{C} - \frac{V_0}{R_L C} \quad (9)$$

Where i_l represents the inductor current, V_0 is the voltage at both ends of the load, I_{pv} and V_{pv} are respectively the current and voltage generated by photovoltaic panel, d is duty ratio of PMW input signal ($d \in [0 \ 1]$), C_r is a filter capacitor, R_L represent resistive load, C and L are respectively capacitor and inductor of the converter.

4. DESIGN OF ADAPTIVE SYNERGETIC MPPT CONTROLLER

An MPPT controller is used to track the MPP generated by the photovoltaic panel during changes in irradiance levels or temperatures. The proposed approach contains two parts:

- P&O maximum power current estimator: a P&O algorithm, as depicted in Figure 6, has been designed to determine the current value at which the photovoltaic panel produces maximum power. This current value denoted as i_{ref} used serves as the set point for the synergetic adaptive loop.
- Synergetic adaptive controller: a controller based on synergetic adaptive estimated by PSO. The asymptotic stability is verified using Lyapunov function to reduce the error between the current estimated i_{ref} and the inductor current i_l . The functionality and design of this controller are illustrated in Figure 7.

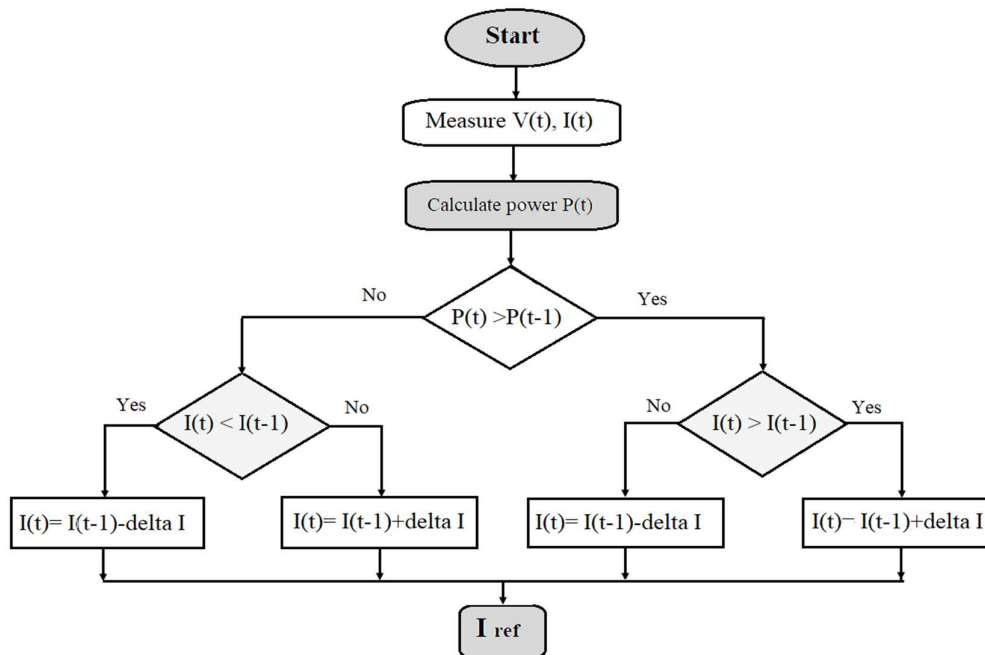


Figure 6. P&O algorithm flowchart

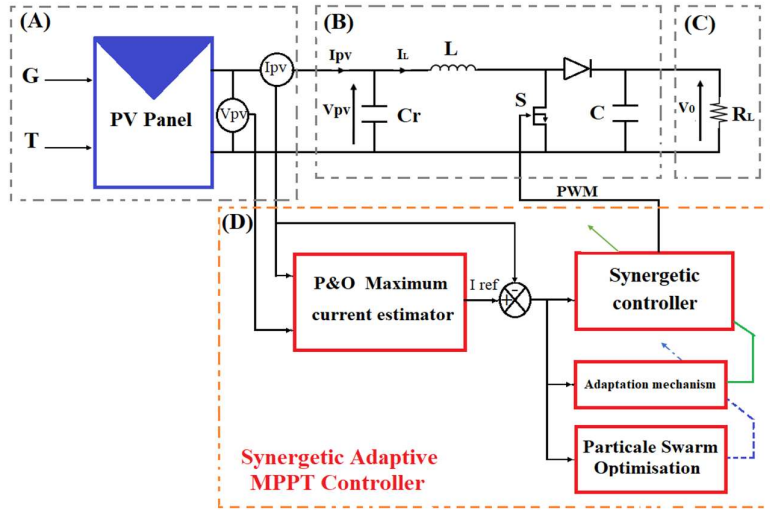


Figure 7. Synergetic adaptive MPPT controller structure

At this stage, the macro-variable of synergetic control is selected as:

$$\Psi = e = i_{ref} - i_L \tag{10}$$

Where the dynamic evolution of the macro-variable is defined as:

$$\Psi + T_s \frac{d\Psi}{dt} = 0 ; T_s > 0 \tag{11}$$

The derivative of the manifold Ψ can be articulated as follows:

$$\frac{d\Psi}{dt} = \frac{de}{dt} = \frac{d(i_{ref} - i_L)}{dt} = \frac{di_{ref}}{dt} - \frac{di_L}{dt} \tag{12}$$

Substituting $\frac{di_L}{dt}$ from (8) into (12):

$$\frac{d\Psi}{dt} = \frac{di_{ref}}{dt} + \frac{V_0}{L} - \frac{V_0}{L} d - \frac{V_{pv}}{L} \tag{13}$$

Incorporate (13) into (11):

$$\Psi + T_s \left(\frac{di_{ref}}{dt} + \frac{V_0}{L} - \frac{V_0}{L} d - \frac{V_{pv}}{L} \right) = 0 \tag{14}$$

The duty cycle is determined as:

$$d = \frac{L}{T_s V_0} \Psi + \frac{L}{V_0} \frac{di_{ref}}{dt} + 1 - \frac{V_{pv}}{V_0} \tag{15}$$

To enhance the efficacy of the algorithm, an adaptive approach is employed to increase the reaction speed. Rather than T_s being a fixed constant, it is adapted to become variable based on the error magnitude.

$$d = \frac{\theta L}{V_0} \Psi + \frac{L}{V_0} \frac{di_{ref}}{dt} + 1 - \frac{V_{pv}}{V_0} \tag{16}$$

With

$$\theta = \frac{1}{T_s} \tag{17}$$

and

$$\tilde{\theta} = \theta - \hat{\theta} \tag{18}$$

Stability analysis and adaptation law. The Lyapunov function is chosen as:

$$V = \frac{1}{2}\psi^2 + \frac{1}{2}\tilde{\theta}^T P^{-1}\tilde{\theta} \quad (19)$$

Its time derivative is

$$\dot{V} = \psi\dot{\psi} + \dot{\tilde{\theta}}^T P^{-1}\tilde{\theta} \quad (20)$$

With the reminder that $\dot{\tilde{\theta}} = -\dot{\hat{\theta}}$, then (20) can be given as:

$$\dot{V} = \psi \left(\frac{d i_{ref}}{dt} - \frac{d i_L}{dt} \right) - \dot{\hat{\theta}}^T P^{-1}\tilde{\theta} \quad (21)$$

Substituting $\frac{d i_L}{dt}$ from (8) into (21):

$$\dot{V} = \psi \left(\frac{d i_{ref}}{dt} + (1-d) \frac{V_0}{L} - \frac{V_{pv}}{L} \right) - \dot{\hat{\theta}}^T P^{-1}\tilde{\theta} \quad (22)$$

Then:

$$\dot{V} = \psi \left(\frac{d i_{ref}}{dt} + \frac{V_0}{L} - \frac{V_0}{L} d - \frac{V_{pv}}{L} \right) - \dot{\hat{\theta}}^T P^{-1}\tilde{\theta} \quad (23)$$

Incorporate (16) into (23)

$$\dot{V} = \psi \left[\frac{d i_{ref}}{dt} + \frac{V_0}{L} - \frac{V_0}{L} \left(\frac{\partial L}{\partial v_0} \psi + \frac{L}{v_0} \frac{d i_{ref}}{dt} + 1 - \frac{V_{pv}}{v_0} \right) - \frac{V_{pv}}{L} \right] - \dot{\hat{\theta}}^T P^{-1}\tilde{\theta} \quad (24)$$

$$\dot{V} = \psi (-\psi \hat{\theta}) - \dot{\hat{\theta}}^T P^{-1}\tilde{\theta} \quad (25)$$

Replacing (18) in (25), \dot{V} becomes:

$$\dot{V} = -\psi^2 (\theta - \tilde{\theta}) - \dot{\hat{\theta}}^T P^{-1}\tilde{\theta} \quad (26)$$

$$\dot{V} = -\psi^2 \theta + (\psi^2 - \dot{\hat{\theta}}^T P^{-1}) \tilde{\theta} \quad (27)$$

So:

$$\dot{V} > 0 \text{ if } \dot{V} = -\psi^2 \theta \quad (28)$$

The adaptation law can be written as:

$$\psi^2 - \dot{\hat{\theta}}^T P^{-1} = 0 \quad (29)$$

Then:

$$\dot{\hat{\theta}} = P\psi^2 \quad (30)$$

Asymptotic stability is verified through Barbalat's lemma. The parameter values of the boost converter, controller, and load are shown in Table 2.

Table 2. System specifications

Parameter	Value
Inductor L	0.225 mH
Capacitor Cr	100 μ F
Capacitor C	100 μ F
Load R _L	12 Ω
Adaptive gain P	0.01

5. SIMULATION RESULTS AND DISCUSSION

This research is concerned with the ongoing challenge of MPP tracking in photovoltaic (PV) systems. While previous studies have made significant contributions in this area, achieving optimum power conversion efficiency remains a critical objective in developing photovoltaic systems. To study the results of the proposed algorithm, a simulation was conducted under standard conditions where the irradiance was 1000 W/m² and the temperature 25 °C. The simulation results are depicted in Figure 8, with several electrical measurements of the PV system shown in Figure 8(a) and the duty cycle displayed in Figure 8(b).

Figure 8 illustrates changes in power, output voltage, generated voltage, and generated current, in addition to the duty cycle, where the response time was estimated at 14 ms. A simulation is now being performed under variable weather conditions where the temperature is kept constant and the irradiance is varied as shown in Figure 9. Figure 10 displays the simulation outcomes, with Figure 10(a) illustrating the PV module responses and Figure 10(b) depicting the duty cycle.

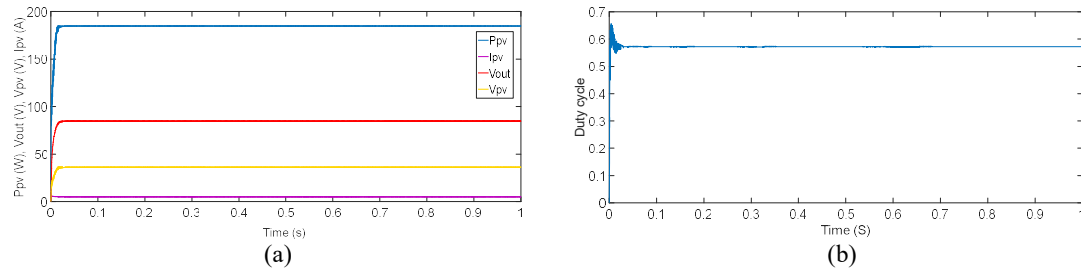


Figure 8. Different responses of the PV module with standard conditions (a) Ppv, Vout, Vpv, Ipv and (b) duty cycle

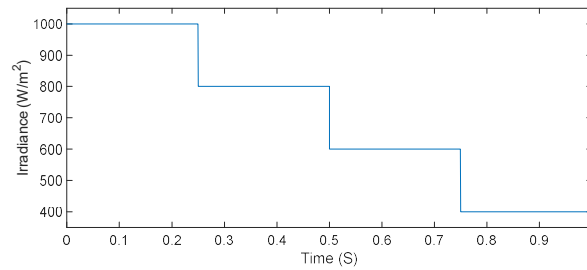


Figure 9. Solar irradiance variation

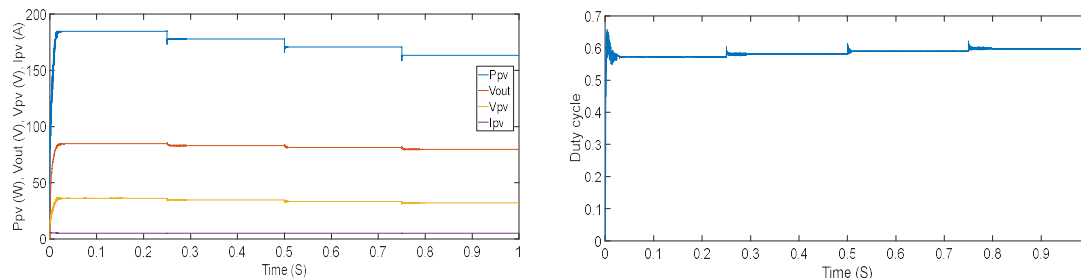


Figure 10. Different responses of the PV module with step irradiance change (a) Ppv, Vout, Vpv, Ipv and (b) duty cycle

The algorithm's response to the sudden change in irradiance was notably rapid, as illustrated in Figure 10, where the maximum power point is tracked in record time. Another simulation is now performed under variable atmospheric conditions where the irradiance is fixed at 1,000 W/m², and the temperature is varied as depicted in Figure 11. The simulation results are presented in Figure 12, with Figure 12(a) showing the various electrical measurements of the PV system, while Figure 12(b) illustrates the duty cycle.

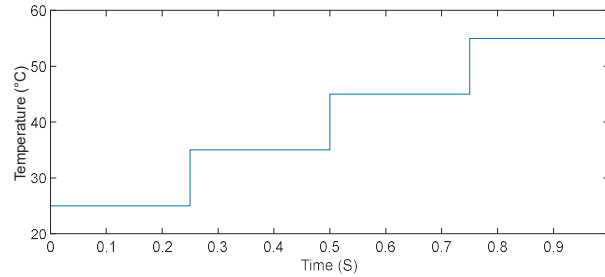


Figure 11. Temperature variation

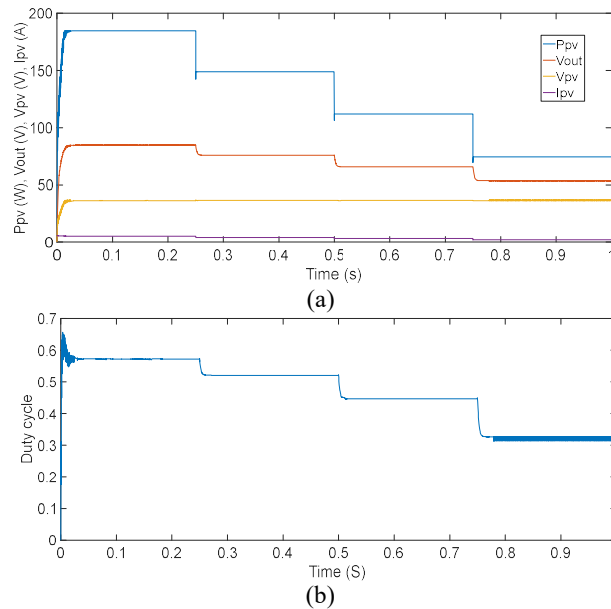


Figure 12. Different responses of the PV module with step temperature change (a) Ppv, Vout, Vpv, Ipv and (b) duty cycle

The effect of temperature change on power conversion was negligible, as the algorithm adeptly tracked the maximum power point within a mere 1 ms. The outcomes demonstrate the proficiency of the employed algorithm in monitoring the maximum power point, even with varying weather conditions. A comparative analysis was performed to validate this effectiveness, contrasting the adopted method with the traditional P&O algorithm. This comparative analysis between the two controllers focused on three aspects: response time, power oscillation and maximum efficiency. The latter is deduced from the following equation [26]:

$$\text{efficiency}(\eta) = \frac{\text{Experiment power}}{\text{Actual power}} \times 100 \quad (31)$$

The simulation results of the comparative study under standard atmospheric conditions are illustrated in Figure 13. The power Ppv, voltage Vpv, current Ipv and output voltage Vout are shown in Figures 13(a)-(d) respectively, while Figure 13(e) shows the duty cycle.

Following a sudden change in weather conditions, characterized by a sudden change in irradiance levels (Figure 9) shown in Figure 14, various electrical measurements are presented. These include power Ppv, voltage Vpv, current Ipv and output voltage Vout shown respectively in Figures 14(a)-14(d), in addition to Figure 14(e) which represents the duty cycle. Then a sudden change in temperature (Figure 11) shown in Figure 15 wherein Figures 15(a)-15(d) display the aforementioned electrical parameters: power Ppv, voltage Vpv, current Ipv, and output voltage Vout, respectively. Figure 15(e) additionally depicts the duty cycle. The effectiveness of each algorithm was assessed with respect to the speed of tracking the maximum power point. The features of each algorithm are summarized in Table 3.

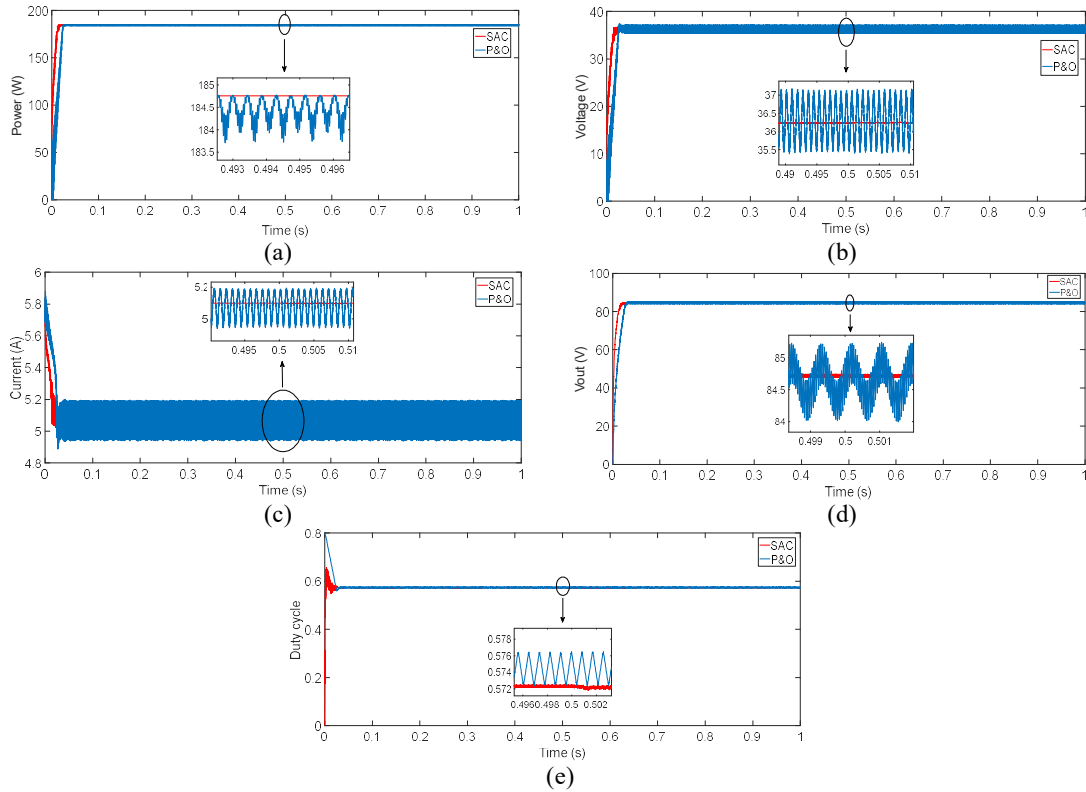


Figure 13. Simulation under standard conditions: (a) P_{pv} , (b) V_{pv} , (c) I_{pv} , (d) V_0 , and (e) duty cycle

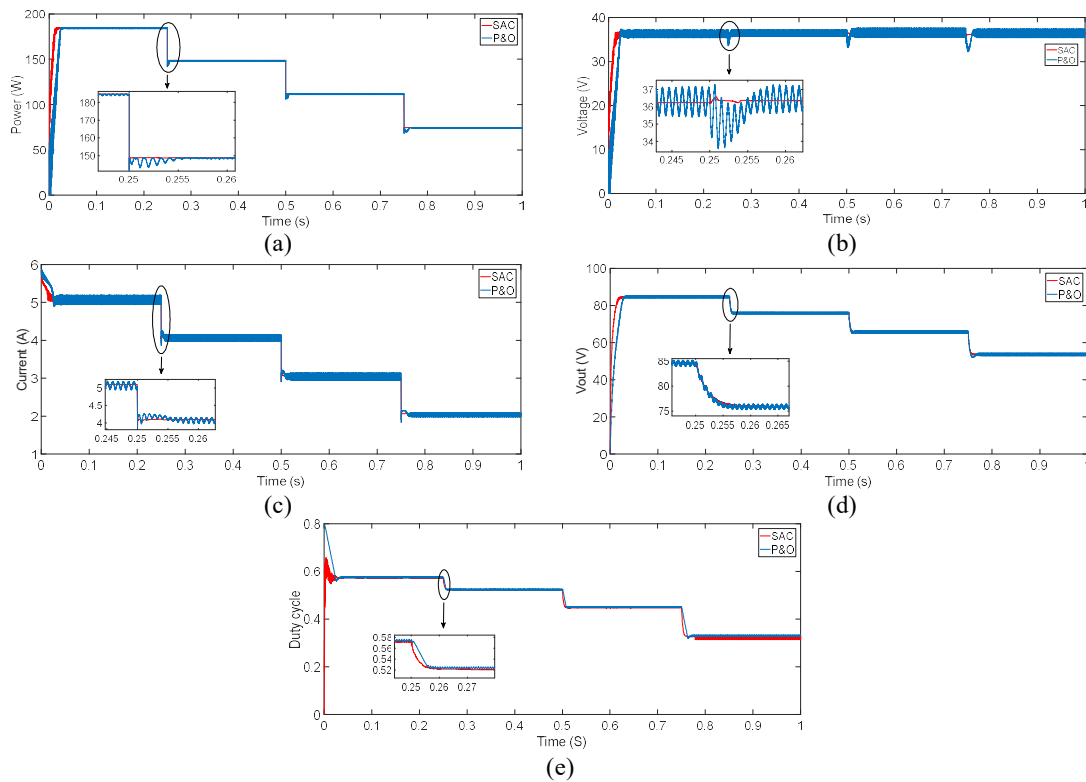


Figure 14. Simulation during rapid irradiance fluctuations: (a) P_{pv} , (b) V_{pv} , (c) I_{pv} , (d) V_0 , and (e) duty cycle

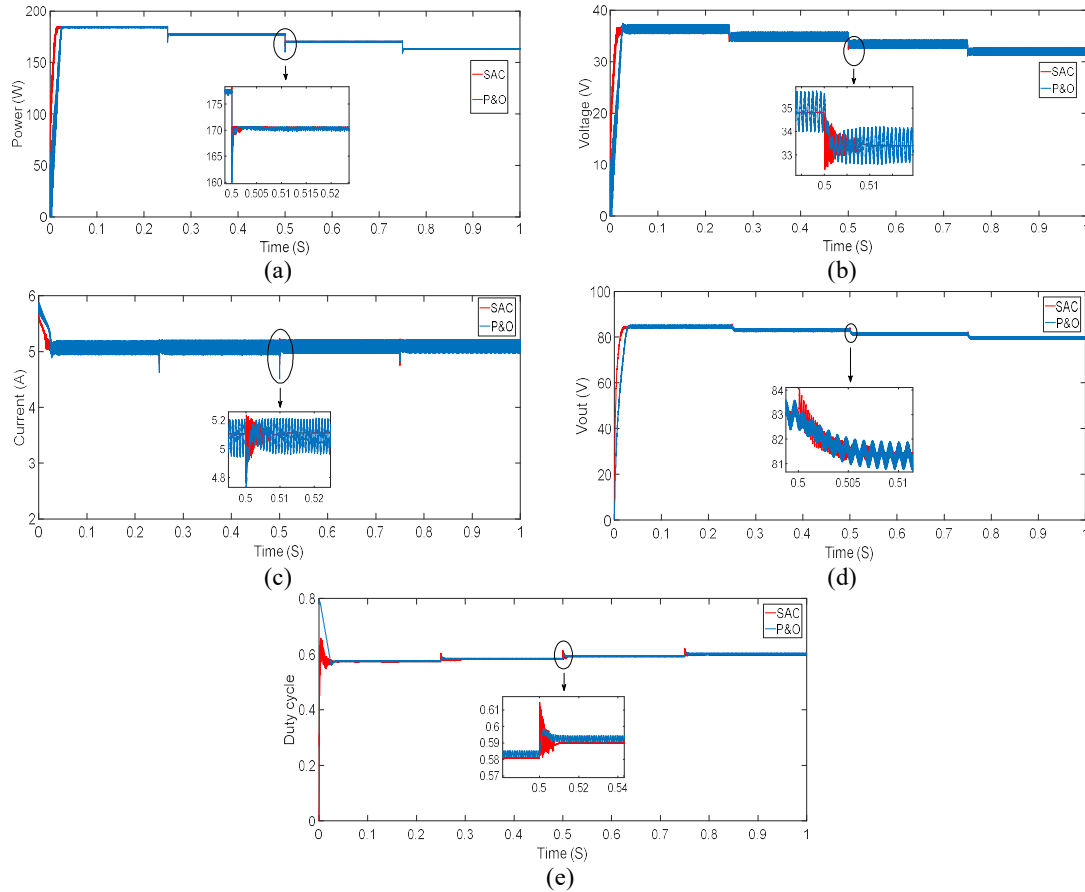


Figure 15. Simulation with step temperature change: (a) P_{pv} , (b) V_{pv} , (c) I_{pv} , (d) V_0 , and (e) duty cycle

Table 3. Performance of the different controllers

MPPT methods	Response time (ms)	Power oscillation (watt)	Max efficiency η (%)
P&O	24	1	98.69
SAC	14	0.001	99.66

Through the simulation results during the standard conditions depicted in Figure 13, it is evident how swift and precise the proposed algorithm is in response, compared to the P&O algorithm. The latter exhibits oscillations in all electrical measurements such as power P_{pv} , output voltage V_{out} , voltage V_{pv} , and current I_{pv} . During the sudden change in irradiance shown in Figure 9, the simulation displayed in Figure 14 demonstrates the reaction speed of the proposed algorithm in tracking the maximum power point compared to the P&O algorithm, across all electrical measurement responses.

As for Figure 15, it portrays the simulation during the sudden temperature change illustrated in Figure 11. The response showcases the capability of the algorithm to swiftly return to the maximum power point compared to the P&O algorithm, across all electrical measurements.

To analyse the results, refer to Table 3, where:

- The SAC controller exhibits a relatively fast response time of 14 ms compared to 24 ms for the P&O.
- Negligible power oscillation for the SAC controller at 0.001 W compared to 1 W for the P&O.
- The efficiency of the SAC controller is higher at 99.66%, compared to 98.69% for the P&O.

The comparative analysis highlighted the superiority of the proposed method in tracking the maximum power point, as illustrated in Table 3, which reveals discernible differences between the SAC controller and the P&O controller with respect to response time, power oscillation and efficiency under changing weather conditions. This study achieved satisfactory results in tracking the maximum power point, especially under varying weather conditions. However, further research is required to address the issue of

partial shading. This is particularly important given the abrupt and unexpected nature of the phenomenon. The results demonstrate the effectiveness of the proposed approach in improving power conversion efficiency. Future research directions include refining the P&O maximum power current estimator to accurately predict the value under partial shading. Recent observations confirm that the proposed algorithm significantly improves energy conversion in photovoltaic systems compared to the P&O algorithm.

6. CONCLUSION

In the current study, a novel MPPT control technique utilizing a synergetic adaptive algorithm has been highlighted. This method has proven effective in maintaining optimal power output from the photovoltaic panel across all climatic conditions, including variations in irradiance and temperature. The photovoltaic system configuration includes a PV panel, a DC-DC boost converter, a resistive load, and a synergetic adaptive controller. The performance and efficacy of the new algorithm were corroborated by simulation outcomes in MATLAB/Simulink, reflecting its competent tracking of the maximum power point under different weather conditions. A comparative analysis with the P&O algorithm was conducted to illustrate the enhancements in power transfer achieved by this algorithm. The study highlights the superiority of the proposed algorithm through faster response times, lower power oscillation, and higher efficiency, indicating significant gains in both efficiency and robustness with the proposed method, which has contributed to the improvement of power conversion in photovoltaic systems. Future work will focus on refining the maximum current estimator to enable prediction of partial shading.




REFERENCES

- [1] K. K. Rout, D. P. Mishra, S. Mishra, S. Patra, and S. R. Salkuti, "Perturb and observe maximum power point tracking approach for microgrid linked photovoltaic system," *IJEECS*, vol. 29, no. 2, pp. 635-643, 2023, doi: 10.11591/ijeeecs.v29.i2.pp635-643.
- [2] N. Femia, G. Petrone, G. Spagnuolo, and M. Vitelli, "Optimization of Perturb and Observe Maximum Power Point Tracking Method," *IEEE Trans. Power Electron.*, vol. 20, no. 4, pp. 963-973, 2005, doi: 10.1109/TPEL.2005.850975.
- [3] S. H. Jacobson and E. Yücesan, "Analyzing the Performance of Generalized Hill Climbing Algorithms," *Journal of Heuristics*, vol. 10, no. 4, pp. 387-405, Jul. 2004, doi: 10.1023/B:HEUR.0000034712.48917.a9.
- [4] A. Zegaoui *et al.*, "Comparison of Two Common Maximum Power Point Trackers by Simulating of PV Generators," *Energy Procedia*, vol. 6, pp. 678-687, 2011, doi: 10.1016/j.egypro.2011.05.077.
- [5] A. Zegaoui, M. Aillerie, P. Petit, J. P. Sawicki, J. P. Charles, and A. W. Belarbi, "Dynamic behaviour of PV generator trackers under irradiation and temperature changes," *Solar Energy*, vol. 85, no. 11, pp. 2953-2964, Nov. 2011, doi: 10.1016/j.solener.2011.08.038.
- [6] F. Bouchafaa, M. Seghir Boucherit, and E. M. Berkouk, "Feedback Loop Control Strategies of the Multi Dc Bus Link Voltages Using Adaptive Fuzzy Logic Control," *Journal of Electrical Engineering*, vol. 64, no. 3, pp. 143-151, May 2013, doi: 10.2478/jee-2013-0021.
- [7] B. Michal, M. J'n, V. Eugen, and F. Peter, "Reducing the Impact of Uncertainties in Networked Control Systems Using Type-2 Fuzzy Logic," *Journal of Electrical Engineering*, vol. 65, no. 6, pp. 364-370, Jan. 2015, doi: 10.2478/jee-2014-0059.
- [8] N. Kacimi, S. Grouni, A. Idir, and M. Seghir Boucherit, "New improved hybrid MPPT based on neural network-model predictive control-kalman filter for photovoltaic system," *IJEECS*, vol. 20, no. 3, pp. 1230-1241, Dec. 2020, doi: 10.11591/ijeeecs.v20.i3.pp1230-1241.
- [9] C. R. Algarín, D. S. Hernández, and D. R. Leal, "A Low-Cost Maximum Power Point Tracking System Based on Neural Network Inverse Model Controller," *Electronics*, vol. 7, no. 1, p. 4, Jan. 2018, doi: 10.3390/electronics7010004.
- [10] M. Mahdavi, L. Li, J. Zhu, and S. Mekhilef, "An adaptive Neuro-Fuzzy controller for maximum power point tracking of photovoltaic systems," *TENCON 2015 - 2015 IEEE Region 10 Conference*, Macao, China, 2015, pp. 1-6, doi: 10.1109/TENCON.2015.7373030.
- [11] T. T. Hoang and T. H. Le, "Application of mutant particle swarm optimization for MPPT in photovoltaic system," *IJEECS*, vol. 19, no. 2, pp. 600-607, Aug. 2020, doi: 10.11591/ijeeecs.v19.i2.pp600-607.
- [12] K. Ishaque, Z. Salam, M. Amjad, and S. Mekhilef, "An Improved Particle Swarm Optimization (PSO)-Based MPPT for PV With Reduced Steady-State Oscillation," in *IEEE Transactions on Power Electronics*, vol. 27, no. 8, pp. 3627-3638, Aug. 2012, doi: 10.1109/TPEL.2012.2185713.
- [13] S. Hadji, J.-P. Gaubert, and F. Krim, "Genetic algorithms for maximum power point tracking in photovoltaic systems," *Proceedings of the 2011 14th European Conference on Power Electronics and Applications*, Birmingham, UK, 2011, pp. 1-9. [Online]. Available: <https://ieeexplore.ieee.org/document/6020380>
- [14] T. Jothi, M. Arun, and M. Varadarajan, "Power flow analysis in a distributed network for a smart grid system," *IJEECS*, vol. 33, no. 1, pp. 42-52, Jan. 2024, doi: 10.11591/ijeeecs.v33.i1.pp42-52.
- [15] Y. Wan, M. Mao, L. Zhou, Q. Zhang, X. Xi, and C. Zheng, "A Novel Nature-Inspired Maximum Power Point Tracking (MPPT) Controller Based on SSA-GWO Algorithm for Partially Shaded Photovoltaic Systems," *Electronics*, vol. 8, no. 6, p. 680, Jun. 2019, doi: 10.3390/electronics8060680.
- [16] S. Mohanty, B. Subudhi, and P. K. Ray, "A New MPPT Design Using Grey Wolf Optimization Technique for Photovoltaic System Under Partial Shading Conditions," in *IEEE Transactions on Sustainable Energy*, vol. 7, no. 1, pp. 181-188, Jan. 2016, doi: 10.1109/TSTE.2015.2482120.
- [17] A. Prabhakaran and A. S. Mathew, "Sliding Mode MPPT Based Control For a Solar Photovoltaic system," *International Research Journal of Engineering and Technology (IRJET)*, vol. 3, no. 6, Jun. 2016.
- [18] H. G. Ali, R. V. Arbos, J. Herrera, A. Tobon, J. P-Restrepo, "Non-Linear Sliding Mode Controller for Photovoltaic Panels with Maximum Power Point Tracking," *Process*, vol. 8, no. 1, p. 108, 2020, doi: 10.3390/pr8010108.
- [19] O. Diouri, A. Gaga, and M. Ouazzani Jamil, "Performance comparison between proportional-integral and backstepping control of maximum power in photovoltaic system," *IJEECS*, vol. 28, no. 2, pp. 744-752, Nov. 2022, doi: 10.11591/ijeeecs.v28.i2.pp744-752.




- [20] B. K. Oubbati, M. Boutoubat, A. Rabhi, and M. Belkheiri, "Experiential Integral Backstepping Sliding Mode Controller to achieve the Maximum Power Point of a PV system," *Control Engineering Practice*, vol. 102, p. 104570, Sep. 2020, doi: 10.1016/j.conengprac.2020.104570.
- [21] H. Attoui, F. Khaber, M. Melhaoui, K. Kassmi, and N. Essounboui, "Development and experimentation of a new MPPT synergetic control for photovoltaic systems," *Journal of Optoelectronics and Advanced Materials*, vol. 18, no. 1–2, pp. 165–173, 2016.
- [22] M. Nadia, F. Grouz, N. Essounboui, and S. Lassaad, "Synergetic MPPT Controller for Photovoltaic System," *Journal of Electrical & Electronic Systems*, vol. 6, no. 2, 2017, doi: 10.4172/2332-0796.1000232.
- [23] H. Kamel, H. Attoui, and A. Djari, "Dynamic Performance Study of an MPPT Controller Using Synergetic Controller for a Photovoltaic System," in *2024 2nd International Conference on Electrical Engineering and Automatic Control (ICEEAC)*, Setif, Algeria: IEEE, May 2024, p. 6. doi: 10.1109/ICEEAC61226.2024.10576505.
- [24] N. Anang, W. M. W. Muda, and M. Z. Daud, "Assessment of a single-phase single-stage grid-connected photovoltaic system," *IJECS*, vol. 30, no. 3, pp. 1339-1347, Jun. 2023, doi: 10.11591/ijeecs.v30.i3.pp1339-1347.
- [25] R. Yauri and R. Espino, "Embedded electronic system for evaluation of photovoltaic modules based on a current-voltage curve tracer," *IJECS*, vol. 29, no. 3, pp. 1281-1289, Mar. 2023, doi: 10.11591/ijeecs.v29.i3.pp1281-1289.
- [26] A. Rawat, S. K. Jha, B. Kumar, and V. Mohan, "Nonlinear fractional order PID controller for tracking maximum power in photovoltaic system," *Journal of Intelligent & Fuzzy Systems*, vol. 38, no. 5, pp. 6703–6713, May 2020, doi: 10.3233/JIFS-179748.

BIOGRAPHIES OF AUTHORS



Kamel Hadjadj    received his Master's degree in Automation in Petrochemical Industries from Skikda University, Algeria. He is currently a PhD student in Automatic and Systems at Setif 1 University, Algeria. His current research interests include power transfer optimization and MPPT control for photovoltaic systems. He can be contacted at email: kamel.hadjadj@univ-setif.dz.



Hadjira Attoui    received her Engineer's degree in Automatic, and her Magister and Doctorate degrees in Automatic, from Setif 1 University, Algeria in 2006, 2009 and 2017, respectively. She is currently a Professor at University Ferhat Abbas-Setif 1 in Setif, Algeria. Her current research interests include process control applications, electrical machines, and photovoltaic systems. She can be contacted at email: attoui_hadjira@univ-setif.dz.